DOI: 10.1002/ejic.200500626

New, Multi-Dimensional Cu(tn)-$[M(CN)_6]^{n-}$ Cyano-Bridged, Bimetallic Coordination Materials (M = Fe^{II}, Co^{III}, Cr^{III} and tn = 1,3-Diaminopropane)

Smail Triki,*[a] Jean Sala-Pala,[a] Franck Thétiot,[a] Carlos J. Gómez-García,[b] and Jean-Claude Daran[c]

Keywords: Bridging ligands / Cyanides / Heterometallic complexes / Magnetic properties

Reaction of the $[Fe^{III}(CN)_6]^{3-}$ anion with $[Cu^{II}(tn)(H_2O)_n]^{2+}$ (tn = 1,3-diaminopropane) affords the compounds $[\{Cu^{II}(tn)\}_2\{Fe^{II}(CN)_6\}]\cdot KCl\cdot 5H_2O$ (**1**), $[\{Cu^{II}(tn)\}_2\{Fe^{II}(CN)_6\}]\cdot 4H_2O$ (**2**), and $[\{Cu^{II}(tnH)_2(H_2O)_2\}\{Fe^{II}(CN)_6\}]\cdot 2H_2O$ (**3**). Each iron center in **1** and **2** is linked to six copper(II) ions by six cyanide bridges, while each copper ion is linked to three equivalent iron(II) ions. Despite these resemblances, the two compounds present large structural differences caused by two different orientations of the Cu–NC–Fe bridges: compound **1** has a 2D structure which can be described as successions of "Cu_4Fe_3" defective cubane units, while compound **2** displays a 3D arrangement. Compound **3**, in which only two *trans*-CN groups are bridging, displays a 1D structure. The tn ligand is chelating in **1**, as is usually observed in several parent compounds, but is unexpectedly a bridging ligand in **2** and a terminal protonated tnH^+ ligand in **3**. Thus, the dimension of the three compounds seems to depend on the tn coordination modes. For the three iron compounds **1**–**3**, the synthetic processes involve the spontaneous reduction of the paramagnetic $[Fe^{III}(CN)_6]^{3-}$ anion into the diamagnetic $[Fe^{II}(CN)_6]^{4-}$ anion. In order to avoid such diamagnetic building blocks, the paramagnetic $[Cr(CN)_6]^{3-}$ anion was used instead of the iron(III) analog, leading to $[\{Cu^{II}(tn)\}_3\{Cr^{III}(CN)_6\}_2]\cdot 3H_2O$ (**4**), which is the first 2D ferromagnet containing "-Cu–NC–Cr-" linkages. A similar study was performed using the diamagnetic $[Co(CN)_6]^{3-}$ anion, leading to $[\{Cu^{II}(tn)\}_3\{Co^{III}(CN)_6\}_2]\cdot 3H_2O$ (**5**), which is the Co analog of **4**. The magnetic properties of compounds **1**–**3** and **5** show the presence of isolated Cu^{II} ions with weak ferromagnetic (**1**) or antiferromagnetic (**2**, **3**, and **5**) interactions. Compound **4** presents a long-range ferromagnetic ordering below T_c = 9.5 K.

Introduction

Bimetallic cyano-bridged assemblies based on polycyanometalates have attracted a great deal of attention because of their remarkable magnetic, photomagnetic, electric-field-induced conductance, catalytic, and porous properties.[1–6] Prussian blue analogs, derived from hexacyanometalate anions and hexa-solvated metal complexes, exhibit novel magnetic and electronic properties, and some of them present magnetic ordering at a critical temperature (T_c) as high as 376 K.[1] However, the difficulty of obtaining crystals suitable for X-ray structure determination precludes a thorough magneto-structural correlation of these 3D systems of high symmetry.[7] In order to tailor their dimensionality and connectivity, and to tune their properties, a different synthetic strategy involving two different families of cyano-bridged coordination assemblies was envisaged. The first family associates $[M(CN)_6]^{n-}$ building-block anions (M = divalent or trivalent first-row transition metal ion) and cationic assembling units of the general formula $[M'L_x(H_2O)_m]^{n+}$ (M′ = divalent first row transition metal ion; L = polyamine, macrocyclic ligand, Schiff base, ...) having selected free coordination sites, instead of simple hexa-solvated complexes;[8–11] the second one involves anionic complexes of general formula $[ML'(CN)_y]^{m-}$ as building blocks instead of the potentially hexadentate $[M(CN)_6]^{n-}$ anions.[12,13] In both families, a large number of such low-symmetry cyano-bridged assemblies display rich and fascinating structural architectures ranging from discrete polynuclear complexes[11,13] to extended 3D networks,[8–10,12] and in some cases exhibit interesting properties such as high T_c magnets, high-spin molecules, or single-molecule magnets. For the first family built on $[M'L_x(H_2O)_m]^{2+}$ and $[M(CN)_6]^{n-}$ units, most of the materials are extended bimetallic compounds having a three- or four-coordinate $[M'L_x]^{2+}$ assembling block which constrains the number of adjacent hexacyanometalate building blocks to two and/or a limited dimensionality of two.[8–10] In contrast, examples in which the assembling block acts as a μ_4-bridging "complex ligand" are very rare. In order to explore such extended bimetallic assemblies with higher connectivities and/or

[a] UMR CNRS 6521, Université de Bretagne Occidentale, B. P. 809, 29285 Brest Cedex, France
Fax: +33-298-017001
E-mail: triki@univ-brest.fr
[b] Instituto de Ciencia Molecular, Universitat de Valencia, Dr. Moliner 50, 46100 Burjasot, Spain
[c] Laboratoire de Chimie de Coordination, UPR CNRS 8241, 205 route de Narbonne, 31077 Toulouse Cedex, France

higher dimensionalities, we decided to focus on the use of two-coordinate assembling units containing the Cu^{II} ion, whose versatility as regards to coordination number and geometry is well known. Reactions of the $[Fe^{III}(CN)_6]^{3-}$ anion with the $[Cu^{II}(tn)(H_2O)_n]^{2+}$ ion (tn = 1,3-diaminopropane) afford the compounds $[\{Cu^{II}(tn)\}_2\{Fe^{II}(CN)_6\}]\cdot KCl\cdot 5H_2O$ (**1**), $[\{Cu^{II}(tn)\}_2\{Fe^{II}(CN)_6\}]\cdot 4H_2O$ (**2**) and $[\{Cu^{II}(tnH)_2(H_2O)_2\}\{Fe^{II}(CN)_6\}]\cdot 2H_2O$ (**3**). Compounds **1**–**3** display 2D, 3D, and 1D structures, respectively, generated by Cu–NC–Fe bridges. For all three compounds the synthetic processes involve the spontaneous reductions of the paramagnetic $[Fe^{III}(CN)_6]^{3-}$ anion into the diamagnetic $[Fe^{II}(CN)_6]^{4-}$ anion, as previously observed for some parent complexes.[14] Therefore, despite the original structural features of these three compounds, their magnetic properties only show weak exchange couplings between Cu^{II} ions through the diamagnetic $[Fe^{II}(CN)_6]^{4-}$ anion. In order to avoid this reduction, the paramagnetic $[Cr(CN)_6]^{3-}$ anion was used instead of the iron(III) analog, leading to the new compound $[\{Cu(tn)\}_3\{Cr(CN)_6\}_2]\cdot 3H_2O$ (**4**), which is the first 2D ferromagnet involving "-Cu–NC–Cr-" linkages. In order to compare with a diamagnetic $[M(CN)_6]^{3-}$ building block, similar attempts were made using the $[Co(CN)_6]^{3-}$ anion; this leads to **5**, the Co^{III} analog of **4**. Herein we report the syntheses, a detailed structural discussion, and the magnetic properties of these five cyano-bridged bimetallic materials. Note that compounds **1** and **4** have recently been briefly communicated by us.[9c,10d]

Results and Discussion

Syntheses and Characterization

The reaction of $CuCl_2$ with $K_3[Fe^{III}(CN)_6]$ and KOH in aqueous solution in the presence of 1,3-diaminopropane (tn) affords $[\{Cu^{II}(tn)\}_2\{Fe^{II}(CN)_6\}]\cdot KCl\cdot 5H_2O$ (**1**) as brown crystals. A similar reaction with $(Et_4N)_3[Fe^{III}(CN)_6]$ and Et_4NOH instead of $K_3[Fe^{III}(CN)_6]$ and KOH results in the formation of $[\{Cu^{II}(tn)\}_2\{Fe^{II}(CN)_6\}]\cdot 4H_2O$ (**2**) as prismatic black crystals. Further concentration of the filtrate afforded $[\{Cu^{II}(tnH)_2(H_2O)_2\}\{Fe^{II}(CN)_6\}]\cdot 2H_2O$ (**3**) as hexagonal, dark-green crystals after several weeks under aerobic conditions. It is likely that the synthetic procedure leading to the slow formation of **3** corresponds to a decrease of the pH by slow aerobic carbonation of the basic solution after several weeks; this allows formation of the tnH^+ unit since the pK_a of the tnH^+/tn couple is around 10.5 (the pH of the solution is about 10.0).[15] Finally, the reaction of $CuCl_2$ and tn with Cr^{III} or Co^{III} hexacyanometalate anions in basic aqueous solution afforded compounds $[\{Cu^{II}(tn)\}_3\{Cr^{III}(CN)_6\}_2]\cdot 3H_2O$ (**4**) and $[\{Cu^{II}(tn)\}_3\{Co^{III}(CN)_6\}_2]\cdot 3H_2O$ (**5**). The crucial role of the base (KOH, Et_4NOH) in these experimental processes must be pointed out: the presence of this base curiously avoids the immediate precipitation of insoluble species and provides the stable two-coordinate aqueous $[Cu(tn)]^{2+}$ unit, which can then react with the hexacyanometalate anions. It is also worthy to note that all the above reactions with $[Fe^{III}(CN)_6]^{3-}$ involve, as shown by the crystal structures and magnetic measurements, its reduction into the diamagnetic $[Fe^{II}(CN)_6]^{4-}$ anion. The reason for this reduction is not clear for the moment. However, on the basis of our observations during this work and careful examination of the literature, we suggest a mechanism that successively involves (i) partial decomplexation of CN^- ligands from the $[Fe^{III}(CN)_6]^{3-}$ complex which, although kinetically inert, is more reactive with regard to ligand substitution than its Fe^{II} analog,[16] (ii) reduction of the aqueous Cu^{II} moiety into the corresponding Cu^{I} unit by the CN^- ions with formation of cyanogen or cyanate,[17] and (iii) reduction of $[Fe^{III}(CN)_6]^{3-}$ into $[Fe^{II}(CN)_6]^{4-}$ by the Cu^{I} species with formation of the Cu^{II} species.[18] Such a $[Fe^{III}(CN)_6]^{3-}$ to $[Fe^{II}(CN)_6]^{4-}$ reduction has been observed previously for some parent M^{II}–L–$[Fe^{III}(CN)_6]^{3-}$ ($M = Cu^{II}$, Ni^{II}, Mn^{II}) systems.[14]

The infrared spectra of **1**–**5** exhibit the bands expected for compounds built from $[Cu(tn)]^{2+}$ and $[M(CN)_6]^{n-}$ units, the presence of the latter being clearly indicated by strong absorption bands assignable to ν_{CN} stretching vibrations in the 2000–2200 cm^{-1} range. Previous studies have shown that the positions of these absorption bands in $[Fe(CN)_6]^{n-}$-containing derivatives can be used as a diagnostic tool for identifying the oxidation state of the metal ion and detecting the presence of cyanide bridges.[19] Terminal CN ligands are typically characterized by absorption bands at around 2120 cm^{-1} when bonded to Fe^{III} and around 2040 cm^{-1} when bonded to Fe^{II}, the shift to lower wavenumbers upon reduction resulting from greater π back-bonding from the Fe^{II} ion to the CN π* antibonding orbital.[20] Coordination of the CN ligand to a second metal ion through its nitrogen atom results in an increase of these values to around 2150–2180 cm^{-1} for $[Fe(CN)_6]^{3-}$ and 2050–2110 cm^{-1} for $[Fe(CN)_6]^{4-}$.[19–21] The ν_{CN} stretching vibrations are found at 2091 and 2079 cm^{-1} for **1** and 2085 and 2056 cm^{-1} for **2**; although unambiguous assignments are difficult, it is likely that these compounds are built from $[Fe^{II}(CN)_6]^{4-}$ units that have their six CN ligands acting as bridging units with Cu ions. For compound **3**, three absorption bands are found at 2095, 2060, and 2032 cm^{-1}; this is in good agreement with the presence of $[Fe^{II}(CN)_6]^{4-}$ units having at last one terminal CN ligand, as indicated by the lower wavenumber band. Similarly, compound **4** exhibits a strong absorption band at 2175 cm^{-1} and two weaker ones at 2149 and 2128 cm^{-1} for the bridging and terminal cyanide groups, respectively. For compound **5**, which contains the $[Co(CN)_6]^{3-}$ unit, the strongest ν_{CN} absorption is observed at 2175 cm^{-1}; the increase of this value with respect to the Fe compound is normal since the CN bond is strengthened as the Co–CN bond involves σ-donation from an antibonding orbital.[22] Finally, the 1,3-diaminopropane ligand is easily characterized by the presence in the IR spectrum of bands due to ν_{NH} stretching vibrations of the NH_2 groups in the 3350–3150 cm^{-1} region and to ν_{CH} stretching vibrations of the CH_2 groups in the 2980–2800 cm^{-1} region.[23a] For compound **3**, the supplementary weak bands observed in the 2700–2500 cm^{-1} region could be tentatively

assigned to ν_{NH} stretching vibrations of the uncoordinated NH_3^+ group.

Crystal Structures

Pertinent bond lengths and angles for compounds **1**–**5** are given in the tables below. Crystallographic data and structure-refinement parameters are given in the Experimental Section.

The crystal structure of compound **1** has been recently communicated;[9c] thus, we limit ourselves to discussing some structural features that are relevant for structural discussion of compound **2** since both present some interesting similarities despite their large structural differences. The asymmetric unit of **1** consists of one $[Fe^{II}(CN)_6]^{4-}$ anion, two $[Cu^{II}(tn)]^{2+}$ cations, one K^+, one Cl^-, and five H_2O molecules, all in general positions. Figure 1 shows an ORTEP drawing of this asymmetric unit with the atom-labeling scheme and the metal-ion environments; pertinent bond lengths and bond angles are given in Table 1. The two nonequivalent copper(II) ions (Cu1 and Cu2) exhibit a CuN_5 geometry (Figure 1), which arises in both cases from two nitrogen atoms of the chelating tn ligand (N7 and N8 for Cu1 and N9 and N10 for Cu2) and from three nitrogen atoms of the cyano groups [N3, N4(f), and N5(d) for Cu1 and N1(a), N2, and N6(c) for Cu2]. The Cu2 ion is located in an approximately square-pyramidal geometry, as indicated by the low value of the trigonality index, τ,[24] of 0.18 [$\tau = (\beta - \alpha)/60$, where α and β are the two greatest basal plane angles ($\beta \geq \alpha$) when the polyhedron is viewed as a square pyramid; for a perfectly square-pyramidal geometry τ is equal to zero, and it becomes unity for a perfectly trigonal bipyramidal geometry. For Cu2, α = N6(c)–Cu2–N10 = 162.3(2)° and β = N2–Cu2–N9 = 173.3(2)°]. This slightly distorted square-pyramidal geometry is in good agreement with the structural data, which indicate that the four equatorial bond lengths are equivalent [Cu2–N2 = 2.005(4), Cu2–N6(c) = 2.008(4), Cu2–N9 = 2.011(4), Cu2–N10 = 2.004(4) Å], while the Cu2–N1(a) apical bond length [2.230(5) Å] is significantly longer. For the Cu1 ion, the corresponding τ value of 0.55 [α = N4(f)–Cu1–N8 = 141.4(2)°, β = N3–Cu1–N7 = 174.2(2)°] indicates that the coordination geometry of the Cu1 ion is intermediate between the two ideal geometries. This coordination geometry can be described as trigonal bipyramidal distorted square-based pyramidal in which one of the equatorial bond lengths is significantly longer [Cu1–N5(d) = 2.122(4) Å] than the other two [Cu–N4(f) = 2.027(6) and Cu1–N8 = 2.039(5) Å] and the apical bond lengths [Cu1–N3 = 2.002(4) and Cu–N7 = 2.009(4) Å].

Each iron ion, which has an almost regular octahedral geometry, is linked to six copper(II) ions by six cyanide bridges, while each copper ion is linked to three equivalent iron(II) ions. The Fe–C–N units are essentially linear while the C–N–Cu angles deviate significantly from linearity (see Table 1). This leads to an infinite $[\{Cu(tn)\}_2\{Fe(CN)_6\}]$ lamellar structure, which can also be described as a 2D layered structure generated by the defective cubane units

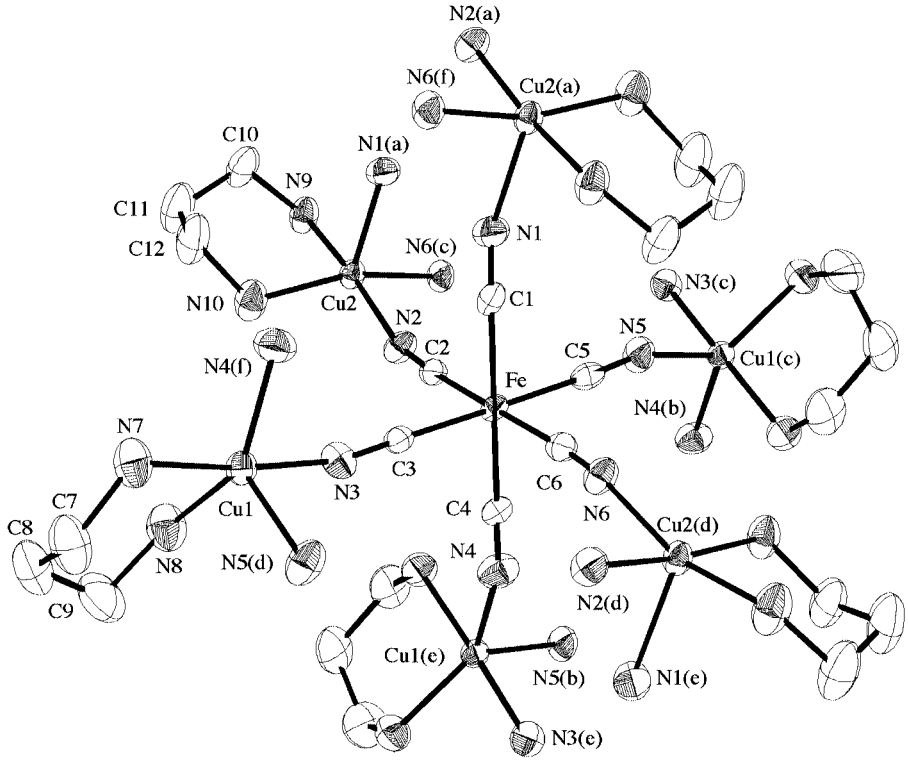

Figure 1. ORTEP view showing the atomic labeling scheme and the metal ion (M = Fe, Cu1 and Cu2) environments in compound **1** (40% probability ellipsoids). Codes of equivalent positions: (a) $-x, -y, 1 - z$; (b) $-x, -y, 2 - z$; (c) $-x, -1/2 + y, 3/2 - z$; (d) $-x, 1/2 + y, 3/2 - z$; (e) $x, 1/2 - y, 1/2 + z$; (f) $x, 1/2 - y, -1/2 + z$.

Table 1. Pertinent bond lengths [Å] and bond angles [°] in compound **1**.

Fe–C–N–Cu	Fe–C	C–N	N–Cu	Fe–C–N	C–N–Cu	Fe···Cu
Fe–C1–N1–Cu2(a)	1.929(6)	1.138(8)	2.230(5)	175.4(4)	156.0(4)	5.194(1)
Fe–C2–N2–Cu2	1.918(5)	1.145(6)	2.005(4)	175.3(5)	161.2(5)	4.980(1)
Fe–C3–N3–Cu1	1.899(4)	1.159(6)	2.002(4)	178.3(4)	162.0(5)	4.997(1)
Fe–C4–N4–Cu1(e)	1.895(6)	1.147(8)	2.027(6)	178.5(4)	160.1(4)	4.991(1)
Fe–C5–N5–Cu1(c)	1.931(4)	1.137(6)	2.122(4)	176.7(5)	159.0(5)	5.114(1)
Fe–C6–N6–Cu2(d)	1.919(5)	1.138(6)	2.008(4)	175.8(5)	163.0(5)	4.998(1)

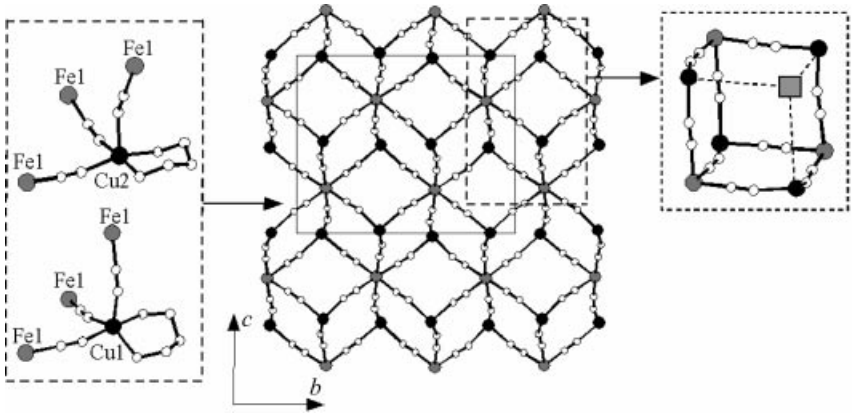

Figure 2. View of the structure of compound **1** showing the 2D arrangement generated by the square-pyramidal units of Cu^{II} and a view of the "Cu_4Fe_3" cubane unit. The chelating tn ligands have been omitted, in the 2D arrangement, for the sake of clarity.

"Cu_4Fe_3", as shown in Figure 2. The distance between two neutral eclipsed parallel sheets is the *a* parameter [15.1478(3) Å], which gives rise to a large interlayer space where the chloride anions, the potassium ions, and the water molecules are accommodated. The shortest Cu···Cu distance is 6.845(1) Å.

Compound **2** crystallizes in the monoclinic system (space group $P2_1/n$); the asymmetric unit consists of one $[Fe^{II}(CN)_6]^{4-}$ anion, located at the special position (0,0,0), one $[Cu^{II}(tn)]^{2+}$ ion, and two H_2O molecules, all in general positions. The copper(II) ion (Cu1) exhibits a CuN_5 geometry (Figure 3) arising from two nitrogen atoms of two equivalent tn ligands (N1, N5) and from three nitrogen atoms of the cyano groups (N11, N12, and N13). As for the Cu1 ion of compound **1**, the corresponding τ[24] value of 0.57 [α = N12–Cu1–N13 = 142.9(2)°, β = N1–Cu1–N5 = 177.0(2)°] indicates that the coordination geometry of the Cu1 ion is a trigonal bipyramidal distorted square-based pyramid with almost equivalent Cu–N bond lengths except for one of the equatorial ones [Cu–N11 = 2.228(4) Å], which is significantly longer than the other four [equatorial: Cu1–N12 = 2.001(4) and Cu1–N13 = 1.987(3) Å; apical: Cu1–N1 = 2.035(3) and Cu–N5 = 2.001(3) Å]. Examination of the N–Cu–N angles in the pseudo base plane [101.8(2), 115.3(2), 142.9(2)°] also indicates that the Cu environment deviates strongly from the ideal trigonal-bipyramidal geometry.

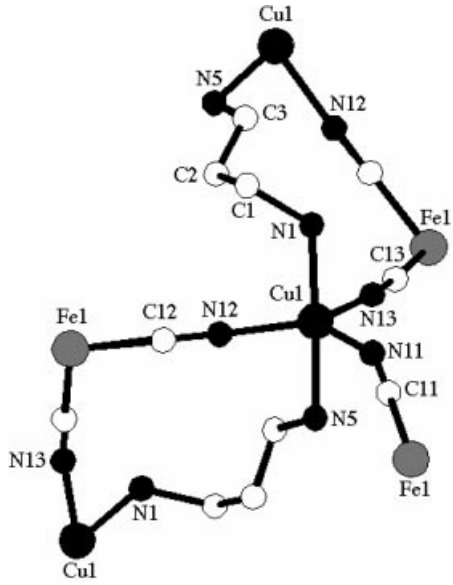

Figure 3. View of the copper ion environment in compound **2**.

As in compound **1**, the iron ion, which has an almost regular octahedral geometry, is linked to six copper(II) ions by six cyanide bridges, while the copper ion is linked to three equivalent iron(II) ions (Figure 4). This leads to a 3D

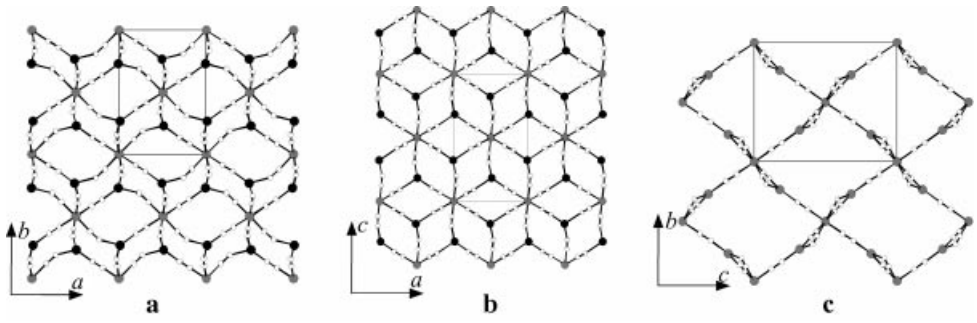

Figure 4. Projections of the structure of compound **2** in the *ab*, *ac*, and *bc* planes. In all cases, the tn ligands have been omitted for the sake of clarity.

Table 2. Pertinent bond lengths [Å] and bond angles [°] in compound **2**.

Fe–C–N–Cu	Fe–C	C–N	N–Cu	Fe–C–N	C–N–Cu	Fe···Cu
Fe1–C11–N11–Cu1	1.930(6)	1.157(6)	2.228(4)	177.5(4)	151.8(4)	5.149(1)
Fe1–C12–N12–Cu1	1.884(5)	1.155(6)	2.001(4)	179.1(4)	175.2(4)	5.036(1)
Fe1–C13–N13–Cu1	1.925(4)	1.154(4)	1.987(3)	177.1(5)	168.4(5)	5.034(1)

arrangement in which the Fe–C–N units are essentially linear, while one of the Cu–N–C units deviates significantly from linearity (Table 2). Careful examination of this 3D arrangement shows two interesting structural features. The first one concerns the projections along the [001] and [010] directions; as shown in Figure 4, they seem to give the same lamellar structure as observed for the 2D structure of **1**. The second one concerns the unexpected coordination mode of the tn ligand; usually chelate, this unit acts in compound **2** as a bridging ligand.

To clearly describe this sophisticated structure, these two structural characteristics are detailed below. The extended structures of compounds **1** and **2** present important structural similarities: (i) they have the same chemical formula $[\{Cu^{II}(tn)\}_2\{Fe^{II}(CN)_6\}]_n$, (ii) in both structures each Cu^{II} ion is linked to three Fe^{II} ions while each Fe^{II} ion is linked to six Cu^{II} ions, and (iii) the projections of **2** along the [001] and [010] directions (parts a, b in Figure 4) seem similar to that of compound **1** along the [100] direction (Figure 2). Despite these common features, large structural differences are observed and the question now is why compound **1** displays a 2D layered structure while the structure of compound **2**, generated only by the cyanide bridges, is 3D. To clarify these differences, the best way seems to be to describe the structural arrangement of **2** on the basis of that of **1**. To simplify such complicated arrangements, the tn ligands are initially omitted. Thus, the extended arrangements of both compounds can be viewed as two different successions of the elemental units depicted in Figure 5 (trigonal pyramid for **1** and trigonal plane for **2**).

For compound **1**, the 2D structure of the "Cu_4Fe_3" defective cubane units depicted in Figure 2 can be easily viewed as a succession of the trigonal-pyramidal units depicted in Figure 5, while for compound **2** the trigonal planes do not allow such a structural arrangement. Thus, the projections of **2** along the [001] and the [010] directions (see a, b in Figure 4) are misleading since they are not appropriate to explain clearly the large differences between the two

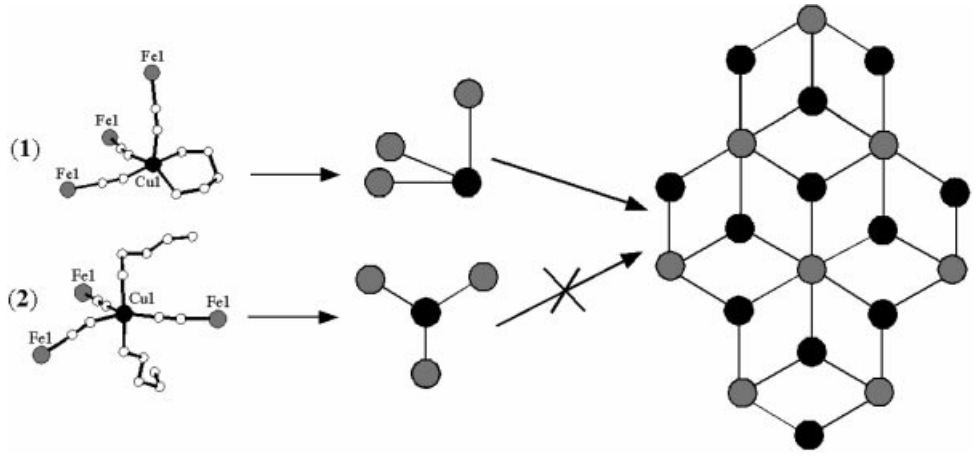

Figure 5. Schematic view showing that the 2D arrangement described as a succession of defective cubane units in compound **1** is not possible in the case of compound **2**.

structural arrangements. A correct description of this 3D arrangement is obtained after rotation of the unreal defective cubane unit around the *a* axis, as shown for this structure in Figure 6 (b); such a rotation shows the real geometry of this unit (Figure 6, c).

The bimetallic cyano-bridged units of **2** differ markedly from the defective cubane units observed in compound **1**, as shown by the schematic view of these units in both compounds (Figure 7).

Slight rotation around the Fe(A)–Fe(A) axis shows a nearly similar view for the structural unit and generates the 2D structure of **1**; the Cu(A) atoms are linked to the Fe(B) atoms by the CN bridges of the same unit leading, as described above, to the 2D structure parallel to the $[Cu(B)]_4$ plane. For compound **2**, a similar slight rotation around the Fe(A)–Fe(A) axis shows that the structural unit is not discrete since the Cu(A) atoms are not linked to Fe(B) atoms as observed for **1**, but linked to the Fe(A) atoms in a third direction that is orthogonal to the $[Cu(B)]_4$ plane. Finally, it is worthy to note that the unusual coordination mode of the tn ligand in compound **2** leads to a helical chain running along the [010] direction with a Cu···Cu distance of 6.719(1) Å (Figure 8). These bridges have no consequences for the structural dimension since compound **2** was described above as having a 3D structure only on the basis of the cyanide bridges.

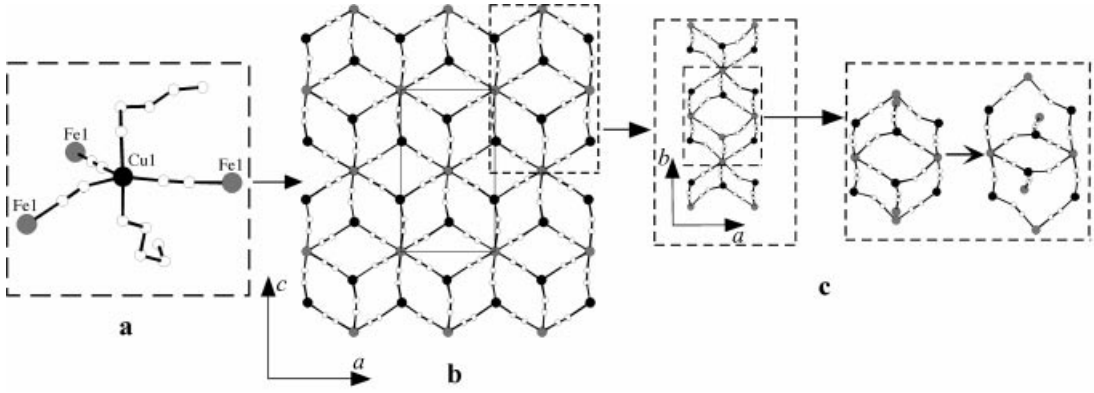

Figure 6. Careful examination of the 3D structure of compound **2**: a) scheme for the copper environment; b) projection of the structure on the *ac* plane; c) the clear structure of fragment unit after rotation around the *a* axis. In (b) and (c), the tn ligands have been omitted for the sake of clarity.

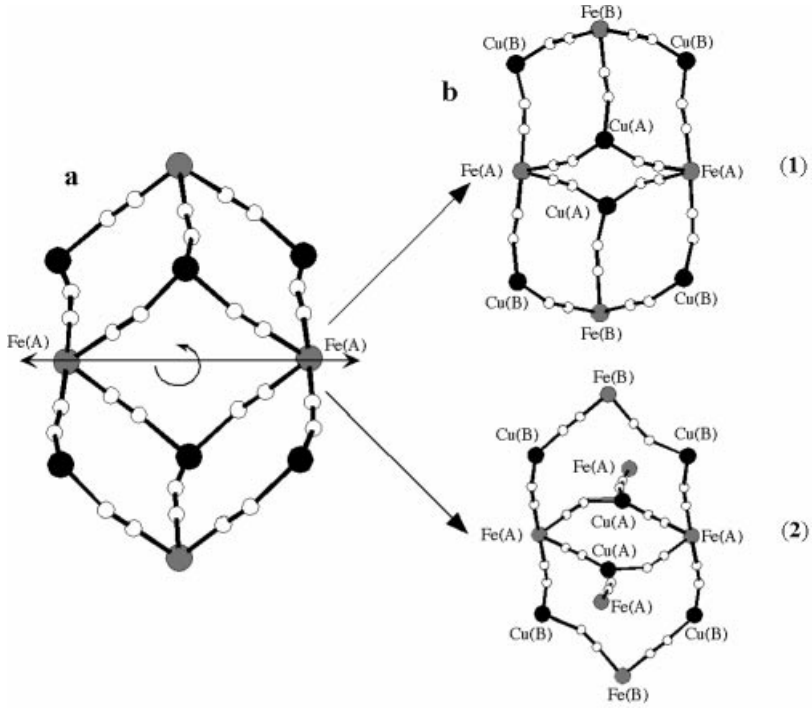

Figure 7. Fragment of the structure showing similarities and differences between compounds **1** and **2**: a) similar projections for both compounds; b) illustration of the structural differences after rotation around the Fe(A)–Fe(A) axis. The tn ligands have been omitted for the sake of clarity. A and B notations are used to indicate more clearly $[Cu(B)]_4$ and the $[Fe(A)]_4$ planes.

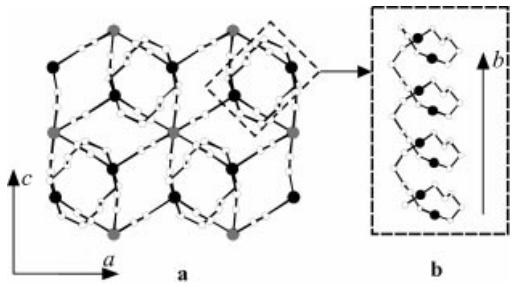

Figure 8. The bridging tn ligand in the 3D structure of compound **2**: a) projection on the *ac* plane; b) the helical chain running along the [010] direction.

Compound **3** crystallizes in the monoclinic system (space group $P2_1/n$); the asymmetric unit consists of one $[Cu(tnH)_2(H_2O)_2]^{4+}$ and one $[Fe(CN)_6]^{4-}$ unit, both localized at special positions[(1/2,0,0) and (0,0,0) respectively], and a water molecule in a general position. Figure 9 shows this asymmetric unit with the atom labeling scheme and the coordination mode of the $[tnH]^+$ ligand. The Cu^{II} ion presents a strongly elongated centrosymmetric CuN_4O_2 environment with four almost equivalent CuN bonds involving two N atoms of CN groups [Cu–N3 and Cu–N3$^{(b)}$: 1.961(4) Å], two N atoms of tn [Cu–N4 and Cu–N4$^{(d)}$: 2.044(4) Å], and two elongated CuO bonds [Cu–O2$^{(e)}$ and Cu–O2$^{(f)}$: 2.633(4) Å] (Figure 10). The Fe^{II} ion presents an almost perfect octahedral FeC_6 coordination [Fe–C bond lengths from 1.914(5) to 1.921(4) Å]. The structure can be described as being formed by linear chains with alternating $[Cu(tnH)_2(H_2O)_2]^{4+}$ and $[Fe(CN)_6]^{4-}$ units linked by a CN bridge (Figure 9). Within a chain, each $[Fe(CN)_6]^{4-}$ is bonded to two Cu ions by two CN groups in a *trans* configuration while each $[Cu(tnH)_2(H_2O)_2]^{4+}$ acts as a μ_2 ligand and not μ_3 as described above for compounds **1**–**2**; the shortest Cu···Fe and Cu···Cu intrachain distances correspond to the *a*/2 and *a* parameter [*a* = 10.0586(4) Å], respectively. It is worthy to note that the tn unit in **3** is protonated; the tnH^+ ligand presents a monodentate coordination mode, with the protonated amine group being uncoordinated (Figure 9).

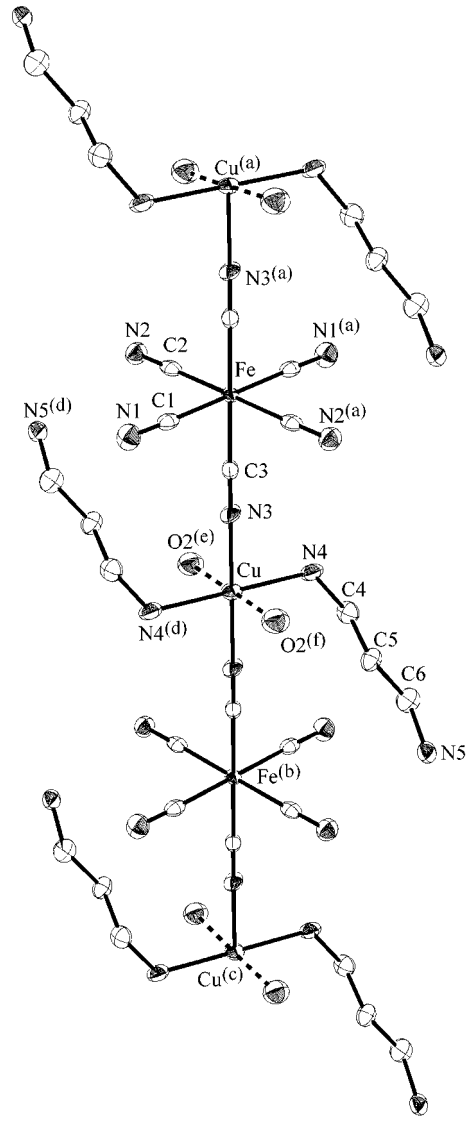

Figure 9. 1D structure of compound **3** showing the atomic labeling scheme and the terminal protonated $[tnH]^+$ ligand (30% probability ellipsoids). Codes of equivalent positions: (a) –*x*, –*y*, –*z*; (b) –1 + *x*, *y*, *z*; (c) 2 – *x*, –*y*, –*z*; (d) –1 – *x*, –*y*, –*z*; (e) –1/2 + *x*, –1/2 – *y*, –1 + *z*; (f) –1/2 – *x*, 1/2 + *y*, 1/2 – *z*.

Compounds **4** and **5** are isostructural and crystallize in the orthorhombic system (space group *Pbcn*). The asymmetric unit contains one $[M(CN)_6]^{3-}$ anion, located at a general position, and two $[Cu(tn)]^{2+}$ (Cu1 and Cu2) ions at special positions (1/2,*y*,1/4). Figure 10 shows an ORTEP drawing of this asymmetric unit with the atom-labeling scheme and the coordination polyhedra of the metal ions; pertinent bond lengths and bond angles of **4** and **5** are given in Table 3. In both structures, the Cu1 atom exhibits a distorted CuN_5 coordination environment (Figure 10) arising from two nitrogen atoms of a chelating tn ligand (N7, N8) and three nitrogen atoms from CN groups [N1, N2(a), and N3$^{(f)}$]. The value of the trigonality index τ[24] is 0.22 for **4** [α = N3$^{(f)}$–Cu1–N7 = 159.2(3)°, β = N1–Cu1–N8 = 172.4(3)°] and 0.20 for **5** [α = N3$^{(f)}$–Cu1–N7 = 159.1(2)°, β = N1–Cu1–N8 = 171.0(2)°]. In agreement with these low values, the coordination geometry of the Cu1 environment can be described in both cases as distorted square-pyramidal, with an apical bond length 0.15–0.18 Å longer than the four equatorial ones. The coordination polyhedron of the Cu2 atom differs strongly from that of Cu1 and can be described as a CuN_4N_2 elongated octahedron generated by a CuN_4 equatorial plane arising from two nitrogen atoms of the chelating tn ligand [N9 and N9(a)] and two equivalent nitrogen atoms of CN groups [N4 and N4(a)], and two axial positions defined by two equivalent nitrogen atoms [N5(b) and N5(c)] of CN groups, the two axial Cu–N5 bond lengths being approximately 0.6 Å longer than the other four in both cases, as shown in Figure 10 and Table 3.

Each M^{III} ion, although bound to six carbon atoms arising from one terminal and five bridging CN ligands, presents an almost regular octahedral coordination geometry, the Cr–C bond lengths being, as usually observed, 0.15–0.18 Å longer than the Co–C ones. In both cases, the ex-

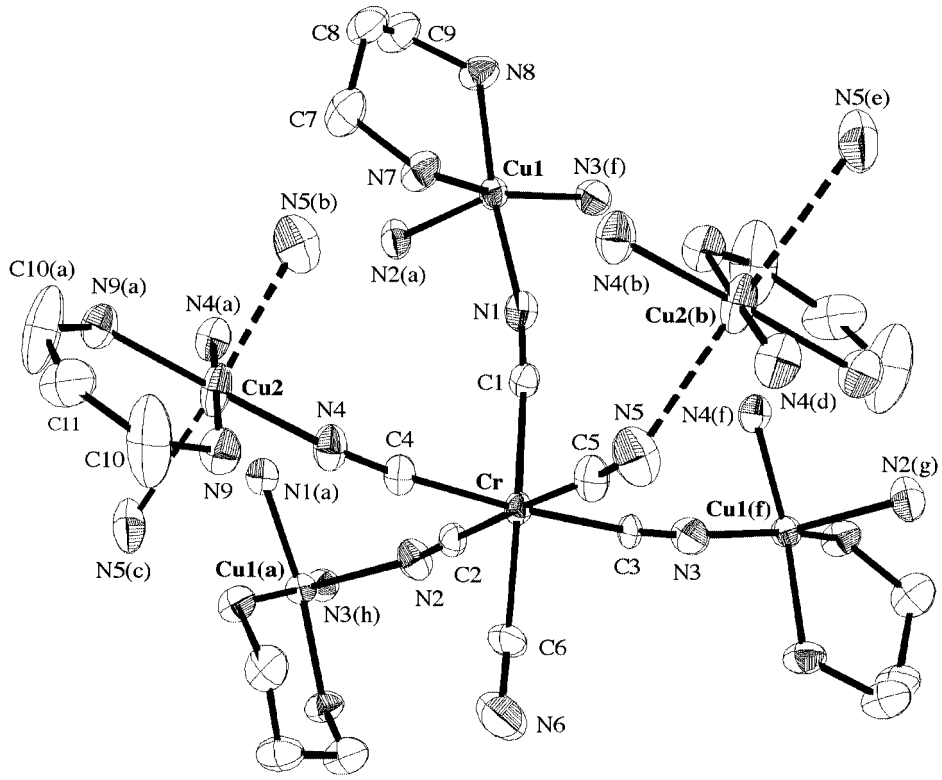

Figure 10. ORTEP view showing the atomic labeling scheme and the metal ion (Cr, Cu1, and Cu2) environments in compound **4** (40% probability ellipsoids). Codes of equivalent positions: (a) 1 – *x*, *y*, 1/2 – *z*; (b) 1 – *x*, 1 – *y*, – *z*; (c) –*x*, 1 – *y*, 1/2 + *z*; (d) *x*, 1 – *y*, –1/2 + *z*; (e) 1 – *x*, *y*, –1/2 – *z*; (f) 1 – *x*, –*y*, –*z*; (g) *x*, –*y*, –1/2 + *z*; (h) *x*, –*y*, 1/2 + *z*.

Table 3. Pertinent bond lengths [Å] and bond angles [°] in **4** and **5**.

M–CN–Cu	M–C	C–N	M–C–N	Cu1–N	Cu2–N	Cu1–N–C	Cu2–N–C	M···Cu
Cr–C1–N1–Cu1	2.047(7)	1.126(9)	173.6(6)	2.014(7)		171.0(6)		5.153(1)
Co–C1–N1–Cu1	1.885(5)	1.141(6)	176.5(4)	1.977(4)		167.2(4)		4.965(1)
Cr–C2–N2–Cu1(a)	2.071(7)	1.144(9)	174.7(6)	2.195(7)		147.9(5)		5.164(1)
Co–C2–N2–Cu1(a)	1.893(5)	1.149(6)	177.0(4)	2.204(4)		145.1(4)		4.989(1)
Cr–C3–N3–Cu1(f)	2.049(6)	1.141(8)	173.7(6)	2.028(6)		172.2(6)		5.187(1)
Co–C3–N3–Cu1(f)	1.893(5)	1.141(6)	175.1(4)	2.011(4)		170.8(4)		5.015(1)
Cr–C4–N4–Cu2	2.042(7)	1.164(8)	173.3(6)		2.005(6)		174.7(6)	5.190(1)
Co–C4–N4–Cu2	1.894(5)	1.135(6)	175.7(5)		2.011(4)		170.7(4)	5.013(1)
Cr–C5–N5–Cu2(b)	2.059(8)	1.14(1)	177.2(7)		2.569(8)		140.0(6)	5.392(1)
Co–C5–N5–Cu2(b)	1.884(5)	1.152(6)	178.5(5)		2.617(5)		140.7(4)	5.312(1)
Cr–C6–N6	2.070(8)	1.12(1)	176.3(10)					
Co–C6–N6	1.888(5)	1.153(7)	177.1(5)					

tended structure can be more clearly described by taking the twelve-membered tetrametallacycle M–CN–Cu–NC–M–CN–Cu–NC as the elemental unit. The molecular arrangement can be seen as a zig-zag "chain" of such "MCuMCu" cycles sharing alternatively one side (Cu1M) and one vertex (Cu1), as shown in Figure 11 (a). The adjacent "chains" are connected to each other through the CN bridges (M–C5–N5–Cu2) to lead to the neutral 2D structure depicted in part b of Figure 11.

As shown in Figure 12, the chelating tn ligands are oriented out of the plane of the bimetallic layers; this imposes a large separation between adjacent layers (adjacent layer distance: *a*/2; shortest Cu–M interlayer distance: ca. 7.0 Å), which is responsible for the presence of the nonbridging C(6)N(6) nitrile group. Careful examination of the 3D structure of $[Mn(en)]_3\{Cr(CN)_6]_2 \cdot 4H_2O$ (**6**), reported by Okawa et al.,[25] shows remarkable structural similarities with the 2D structures of **4** and **5**. Despite important differ-

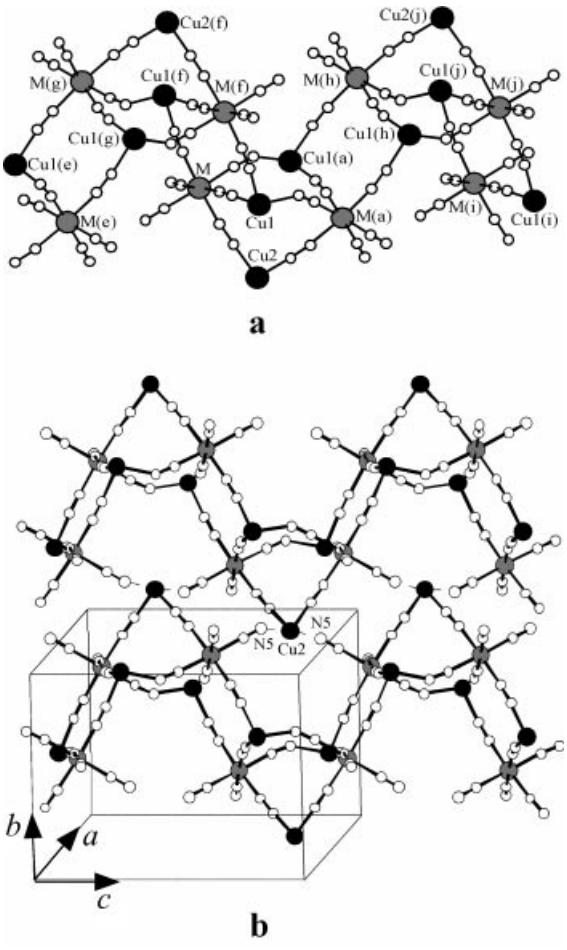

Figure 11. Structure of compounds **4** and **5**: a) schematic view of a zigzag chain unit; b) 2D arrangement. The tn chelating ligands have been omitted for clarity. Codes of equivalent positions: (a) 1 – *x*, *y*, 1/2 – *z*; (e) 1 – *x*, *y*, –1/2 – *z*; (f) 1 – *x*, –*y*, –*z*; (g) *x*, –*y*, –1/2 + *z*; (h) *x*, –*y*, 1/2 + *z*; (i) *x*, *y*, 1 + *z*; (j) 1 – *x*, –*y*, 1 – *z*.

ences related essentially to their dimensionalities, the 3D structure of **6** can be easily described from the 2D structure of **4** and **5** by taking into account that the cyano group, which is terminal in the latter [C(6)N(6)], adopts a bridging coordination mode in **6** (see Figures 10 and 12). This supplementary cyano bridge may be explained by the presence of the en ligand in **6**, which has a lower steric hindrance than the tn ligand.

Magnetic Properties

The magnetic properties for compounds **1**–**3** and **5** are displayed in Figure 13 as the thermal variation of the $\chi_m T$ product (χ_m being the molar magnetic susceptibility per formula unit). Compounds **2**, **3**, and **5** show similar behaviors, with a constant $\chi_m T$ value from room temperature down to low temperatures (20–30 K); below this temperature, they show smooth decreases of the $\chi_m T$ product due to weak antiferromagnetic interactions between Cu^{II} ions through the diamagnetic hexacyanometalate building block anions in the d^6 low-spin configuration {$[Fe^{II}(CN)_6]^{4-}$ for compounds **2** and **3** and $[Co^{III}(CN)_6]^{3-}$ for compound **5**}. Compound **1** displays the same behavior in the high-temperature range but shows an increase in the $\chi_m T$ value at low temperatures, which is characteristic of weak, but significant, ferromagnetic interactions between Cu^{II} ions through the diamagnetic building block anion.

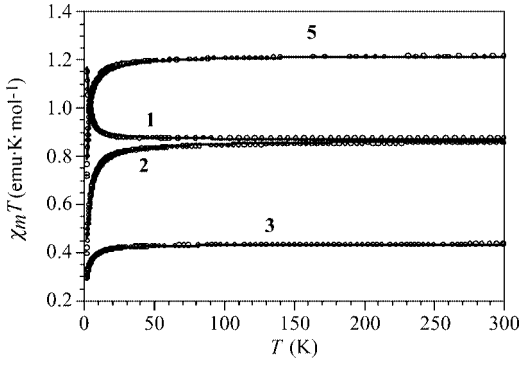

Figure 13. Thermal variation of $\chi_m T$ for compounds **1**, **2**, **3**, and **5**. Solid lines are the best fits to the Curie–Weiss law (see text).

These behaviors indicate that the four compounds behave essentially as paramagnets with weak Cu^{II}–Cu^{II} magnetic

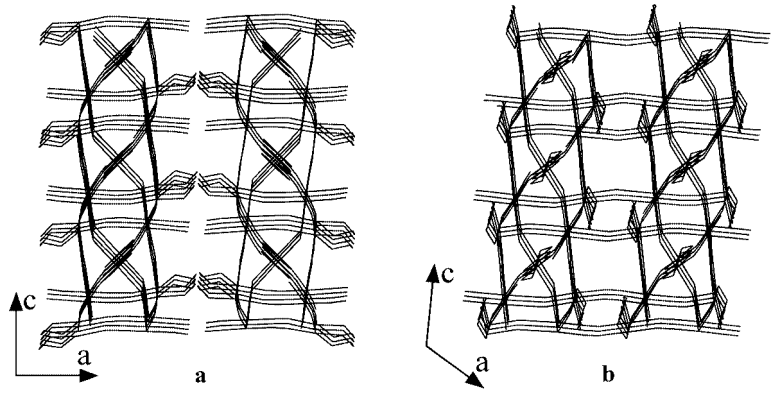

Figure 12. a) Schematic view of two adjacent layers in compounds **4** and **5** showing the nonbridging CN groups and the chelating tn ligands; b) view of the 3D arrangement of compound **6** (obtained from crystal data given in the cif file of ref.[25]); the nonbridging CN group observed in **4** and **5** is bridging here.

interactions, as expected from the structural data that show that the Cu^{II} ions are quite well isolated due to the diamagnetic building blocks that preclude the existence of significant exchange interactions between the Cu^{II} ions. Thus, for each of these four compounds, the magnetic data can be very well reproduced with a simple Curie–Weiss law: $\chi_m = C/(T - \theta)$. In all cases, this expression gives a very satisfactory agreement with the experimental data in the whole temperature range (solid lines in Figure 13) with the sets of parameters displayed in Table 4; these results corroborate the presence of weak ferromagnetic interactions in **1** and weak antiferromagnetic interactions in **2**, **3**, and **5**.

Table 4. Magnetic parameters for compounds **1**–**3** and **5**.

	Cu^{II}_nM	C [emu K mol^{-1}]	g	Θ [K]
1	$Cu^{II}_2Fe^{II}$	0.869(1)	2.152	+0.515(3)
2	$Cu^{II}_2Fe^{II}$	0.866(1)	2.149	–1.76(2)
3	$Cu^{II}Fe^{II}$	0.435(1)	2.153	–0.97(2)
5	$Cu^{II}_3Co^{III}$	1.218(3)	2.081	–0.98(2)

A confirmation of the spin ground-state and the weak magnetic interactions in compounds **1**, **2**, **3**, and **5** comes from the isothermal magnetization of these compounds at 2 K. In all cases, the magnetization can be well reproduced with a Brillouin function for one (**3**), two (**1** and **2**), or three (**5**) independent $S = 1/2$ ions with reduced (**2**, **3**, and **5**) or increased (**1**) g values accounting for the weak interactions observed at low temperatures. The magnetic behavior of **1** is similar to that observed in the previously reported compound $[Cu^{II}(en)(H_2O)\}_2\{Fe^{II}(CN)_6]\cdot 4H_2O$, which contains Cu–NC–$Fe^{II}$–CN–Cu bridges.[23b] In this compound, the nature of the ferromagnetic coupling was explained as having two possible origins: (i) intrachain interactions through the diamagnetic -NC–Fe^{II}–CN- bridges, or (ii) interchain interactions through double end-on cyanide bridges. As shown above, the crystal structure of **1** involves infinite 2D sheets that are eclipsed and about 15.0 Å apart. This large distance means that the adjacent sheets are well isolated and precludes consideration of any inter-sheet interaction. Thus, the weak magnetic coupling in **1** can be attributed to the interaction between Cu^{II} ions through the diamagnetic -NC–Fe^{II}–CN- bridges. Note that such an assignment needs more experimental support but examples involving extended and discrete cyano-bridged compounds with similar diamagnetic -NC–M–CN- bridges (M = Fe^{II} in $[Fe(CN)_6]^{4-}$, M = Fe^{III} in $[Fe(CN)_5(NO)]^{2-}$, and M = Co^{III} in $[Co(CN)_6]^{3-}$) between Cu^{II} ions are very rare.[13e,23,26,27] However, such diamagnetic bridges lead to the same situation in some Ni^{II}–Fe^{II} and Mn^{II}–Fe^{II} bimetallic compounds;[14a,14b,26d,28] taking into consideration the electronic configuration of $Ni^{II}(t_{2g}^6e_g^2)$ or Mn^{II} $(t_{2g}^3e_g^2)$ and Fe^{II} $(t_{2g}^6e_g^0)$, a σ-superexchange pathway between Ni^{II} (or Mn^{II}) ions through the empty d_σ orbital of the Fe^{II} ion was proposed to explain the ferromagnetic exchange coupling. Thus, it seems likely that a similar ferromagnetic behavior occurs in compound **1** even if the Cu^{II} ion presents a nonoctahedral environment. Consequently, such ferromagnetic behavior should also occur in compounds **2** and **3** instead of the weak antiferromagnetic or the paramagnetic behavior actually observed. For compound **5**, which also involves diamagnetic bridges between Cu^{II}, the weak antiferromagnetic behavior observed is similar to those of a few examples recently reported.[27] Finally, on the basis of this study and on some reported examples involving diamagnetic -NC–M–CN- bridges between Cu^{II} ions, we can conclude, as expected from the structural data (Cu···Cu ≥ 6.7 Å), that weak magnetic interactions occur through such diamagnetic bridges. In contrast, a clear exchange mechanism concerning the nature of the magnetic coupling needs more examples of M–Cu^{II} cyano-bridged bimetallic compounds.

As expected, substitution of the diamagnetic $[Co(CN)_6]^{3-}$ anion by the paramagnetic $S = 3/2$ $[Cr(CN)_6]^{3-}$ anion results in a drastic modification of the magnetic properties, as will be shown below. The thermal variation of the molar magnetic susceptibility (χ_m) of compound **4** shows an abrupt increase below about 15 K (maximum slope at about 11 K) followed by an almost saturation at low temperatures (Figure 14). This behavior suggests the presence of a long-range ordering in this compound below about 10 K. The thermal variation of the $\chi_m T$ product (per "Cu_3Cr_2" formula unit) shows a room-temperature value of about 5.0 emu K mol^{-1}, which is close to the expected value (4.875 emu K mol^{-1}) for three noninteracting Cu^{II} ($S = 1/2$) and two Cr^{III} ($S = 3/2$) ions with $g = 2$ (inset in Figure 14). On cooling the sample, the $\chi_m T$ product shows a continuous increase, which is indicative of a ferromagnetic coupling between the Cr^{III} and Cu^{II} ions in **4**. In fact, the magnetic susceptibility of **4** follows a Curie–Weiss law above about 100 K with $C = 4.97(1)$ emu K mol^{-1} and $\theta = +46.0(2)$ K; note that the positive sign of θ confirms the presence of dominant ferromagnetic interactions between neighboring Cr^{III} and Cu^{II} ions. On cooling the sample further, the $\chi_m T$ product shows a maximum of about 58 emu K mol^{-1} at about. 11 K; below this temperature the $\chi_m T$ product decreases sharply, due to saturation effects of the χ_m at low temperatures, to reach a value of around 15 emu K mol^{-1} at 2 K (inset in Figure 14).

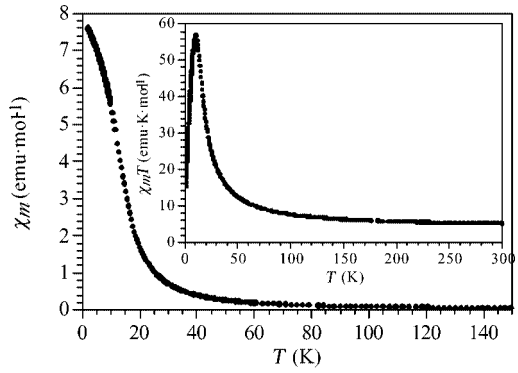

Figure 14. Thermal variations of χ_m and $\chi_m T$ (inset) for compound **4**.

To confirm the ferromagnetic nature of the long-range order transition and to determine the exact transition temperature, we performed magnetic susceptibility measure-

ments in an alternating field (AC susceptibility, Figure 15). These measurements show: (i) a frequency-independent peak at about 9.0 K and an additional frequency-dependent shoulder at lower temperatures in the in-phase susceptibility (χ'_m) ,and (ii) a non-zero frequency-independent out-of-phase susceptibility (χ''_m) below about 9.5 K that presents a frequency-dependent broad maximum at lower temperatures (3.6–4.7 K). From these data, we can conclude that compound **4** presents a ferromagnetic long-range ordering and that the ordering temperature is about 9.5 K. Furthermore, the presence of the frequency-dependent shoulders (in χ'_m) and broad maxima (in χ''_m) suggests that the movement of the domain walls in the ferromagnetically ordered phase is strongly hindered below about 5 K. A possible explanation is that the magnetic transition at 9.5 K corresponds to a ferromagnetic ordering within the layer (which is frequency independent, as observed in the χ'_m peak at about 9.0 K), and that at lower temperatures (below ca. 5 K) the dipolar coupling induces a 3D ferromagnetic ordering in which the domain walls are anchored.

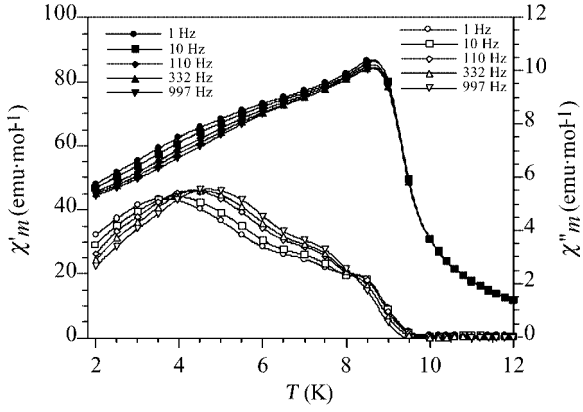

Figure 15. Thermal variation of the in-phase (χ'_m, filled symbols, left scale) and out-of-phase (χ''_m, empty symbols, right scale) signals of compound **4** at 1, 10, 110, 332, and 997 Hz (circles, squares, rhombs, up-triangles and down-triangles, respectively).

In this case, the frequency dependence of χ'_m can be related to the activation energy required to unlock these domain walls. This activation energy (E_a) can be deduced from the frequency dependence of the maximum of χ''_m, which follows an Arrhenius la w, as E_a = 112(2) K. An additional proof comes from the fact that the application of increasing DC fields in the AC measurements reduces the shoulder in χ'_m and the broad maximum in χ''_m; both features disappear when the DC field is above about 100 mT (Figure 16). Furthermore, the temperature of these two features decreases as the DC field increases (Figure 16), indicating, as expected, that the magnetic field helps the unlocking of the domain walls. A very similar behavior has recently been observed in $[Ni(trans\text{-}C_6H_{14}N_2)_2]_3\{Fe(CN)_6]_2\cdot 2H_2O$, a similar layered cyanide-bridged bimetallic ferromagnet (T_c = 14.0 K, E_a = 111.6 K) with the same stoichiometric M^{II}_3-M^{III}_2 ratio[8g] and in the two pure enantiomeric derivatives of the same compound obtained with *trans*-(1*S*,2*S*)-$C_6H_{14}N_2$ and *trans*-(1*R*,2*R*)-$C_6H_{14}N_2$ (T_c = 13.8 K, E_a = 156 K).[8h] Note that the ordering temperature of **4** (T_c = 9.5 K) is lower than that reported for the 3D compound $[Cu(EtOH)_2][Cu(en)]_2\{Cr(CN)_6]_2$ (T_c = 57 K),[10e] which was previously the only known example of a cyano-bridged Cu_3Cr_2 ferromagnet. The difference in the ordering temperature can be related to the lower dimensionality and/or to the lower Cr–Cu exchange interactions of **4** as a result

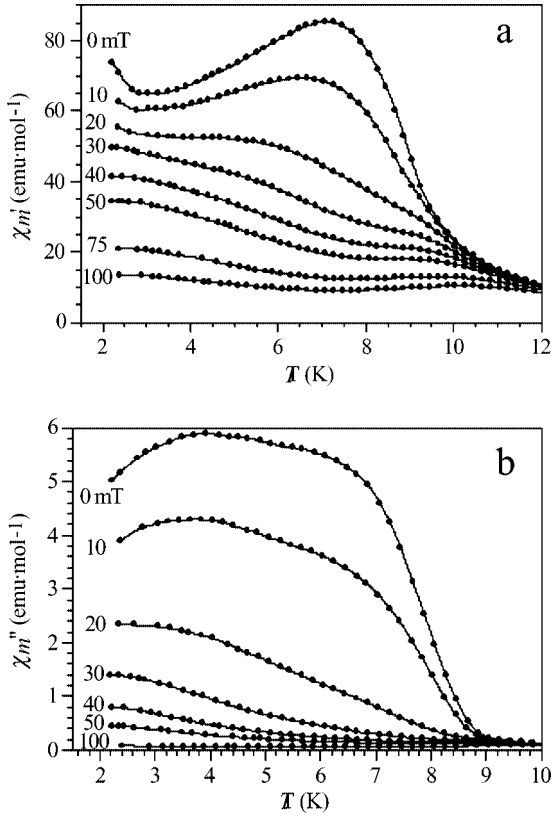

Figure 16. Thermal variation of the in-phase (a) and out-of-phase (b) signals of compound **4** at 3000 Hz with different applied DC magnetic fields.

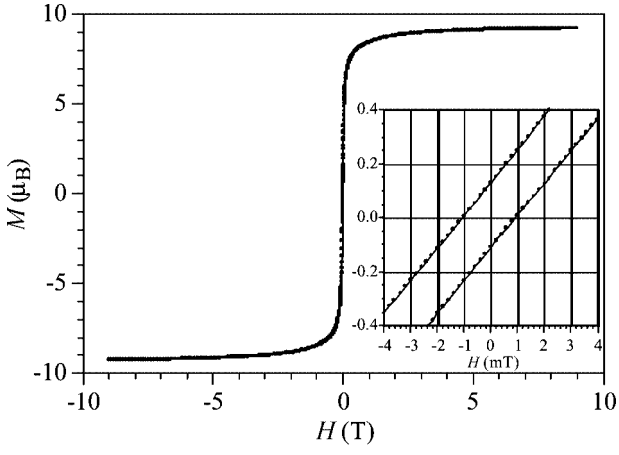

Figure 17. Hysteresis cycles at 2 K for compound **4**. The inset shows the low-field region.

of the different Cu–CN–Cr angles observed in both compounds.

An additional proof of the ferromagnetic nature of the long-range ordering comes from the isothermal magnetization of **4** at 2 and 5 K, which shows (i) a rapid saturation of the magnetization for magnetic fields above about 0.5 T (Figure 17), (ii) a saturation value of around 9.2 μ_B, which is the expected value for the parallel alignment of three $S = 1/2$ plus two $S = 3/2$ spins with a g value close to 2, and (iii) a hysteresis with small and similar coercive fields of 1.0 mT at 2 and 5 K, indicating that **4** is a soft ferromagnet.

Conclusions

This study involves the design of some new bimetallic materials that contain a hexacyanometalate $[M(CN)_6]^{n-}$ ion and a two-coordinate $[CuL]^{2+}$ unit (L = $H_2NCH_2CH_2CH_2NH_2$). With $[Fe(CN)_6]^{3-}$, spontaneous Fe reduction was observed to afford the $[Fe(CN)_6]^{4-}$ ion. This diamagnetic building block leads to three new Cu–Fe combinations corresponding to different diamine coordination modes: chelating, bridging, and terminal, with protonation of one of the NH_2 groups. These three bimetallic compounds, for which magnetic properties only show weak exchange couplings between Cu^{II} ions through diamagnetic hexacyanometalate bridges, have original 1D or 2D structures whose dimensionalities seems to be related to the coordination mode of the diamine unit. In order to obtain interesting magnetic behavior with paramagnetic building blocks, similar studies were performed using the $S = 3/2$ $[Cr(CN)_6]^{3-}$ building block; this leads to the first 2D ferromagnet involving Cr–CN–Cu linkages. Despite important differences related essentially to their dimensionality, this compound, $[Cu(H_2NCH_2CH_2CH_2NH_2)\}_3\{Cr(CN)_6]_2 \cdot 3H_2O$, and the recently reported $[Mn(H_2NCH_2CH_2NH_2)][Cr(CN)_6]\cdot 4H_2O$ show some remarkable structural similarities. These results, associated with some others already reported in the literature, show the ability of the $[M(CN)_6]^{n-}/[CuL]^{2+}$ system to afford a wide variety of bimetallic combinations depending not only on the nature of M and L but also on other parameters such as the pH and the nature of the counteranions. Extension of this study to other amine ligands and to other experimental conditions is in progress in order to obtain a more unified view of the structural data/magnetic behavior relationship in these bimetallic combinations.

Experimental Section

General: All reagents were purchased from commercial sources and used as received. $(Et_4N)_3[Fe^{III}(CN)_6]$ and $(Et_4N)_3[Co^{III}(CN)_6]$ were prepared from the corresponding potassium hexacyanometalate in two steps via the corresponding silver salt with a procedure adapted from that reported by Le Magueres,[29] using acetonitrile as solvent instead of water. Elemental analyses were obtained from the Service Central d'Analyses (Vernaison) and Service de Micro-analyses de ICSN-CNRS (Gif-sur-Yvette). Infrared spectra were recorded in the range 4000–200 cm^{-1} as KBr pellets on a FT-IR Nexus Nicolet spectrometer. Variable temperature susceptibility measurements were carried out in the temperature range 2–300 K with applied magnetic fields of 0.1 T on polycrystalline samples for all the compounds with a Quantum Design MPMS-XL-5 SQUID magnetometer. The susceptibility data were corrected for the sample holders previously measured using the same conditions and for the diamagnetic contributions of the salt, as deduced by using Pascal's constant tables. For **4**, the AC susceptibility measurements were performed in the temperature range 2–20 K with an alternating field of 0.395 mT at different frequencies in the 1–1000 Hz range with the SQUID susceptometer and with an alternating field of 1.7 mT at different frequencies in the 1–10 kHz range applying different DC magnetic fields (between 0 and 100 mT) with a Quantum Design Physical Properties Measurement System, PPMS-9.

Synthesis of $[\{Cu^{II}(tn)\}_2\{Fe^{II}(CN)_6\}]\cdot KCl\cdot 5H_2O$ (1) (tn = 1,3-diaminopropane): This compound was prepared as brown crystals by a procedure similar to that given below for **2**, from $K_3[Fe^{III}(CN)_6]$ (0.66 g, 2.0 mmol) and KOH (0.67 g, 12.0 mmol) instead of $(Et_4N)_3[Fe^{III}(CN)_6]$ and Et_4NOH. This procedure and the analytical and IR data of **1** have been previously communicated.[9c] Yield: 0.52 g (40%).

Synthesis of $[\{Cu^{II}(tn)\}_2\{Fe^{II}(CN)_6\}]\cdot 4H_2O$ (2) and $[\{Cu^{II}(tnH)_2(H_2O)_2\}\{Fe^{II}(CN)_6\}]\cdot 2H_2O$ (3): 1,3-Diaminopropane (1.0 mL, 12.0 mmol) was added under aerobic conditions to a concentrated aqueous solution (5 mL) of $CuCl_2\cdot 2H_2O$ (2.05 g, 12.0 mmol) with continuous stirring, leading to the immediate precipitation of a green powder. An aqueous solution of Et_4NOH (0.52 g, 3.5 mmol) was then added with stirring and the resulting dark-blue solution was warmed (ca. 60 °C for about 5 min) and then filtered in order to remove the small amount of precipitate that remained. An aqueous solution (20 mL) of $(Et_4N)_3[Fe^{III}(CN)_6]$ (3.62 g, 6.0 mmol) was then added with continuous stirring. Slow concentration of the resulting solution at room temp. afforded prismatic black crystals of **2**, which were filtered and air-dried. Further evaporation afforded hexagonal dark green crystals of **3** after several weeks under aerobic conditions; these were filtered and air-dried.

2: Yield: 0.84 g (25%). $C_{12}H_{28}Cu_2FeN_{10}O_4$ (559.38): calcd. C 25.77, H 5.05, Cu 22.72, Fe 9.98, N 25.04; found C 25.68, H 5.02, Cu 22.61, Fe 9.85, N 25.13. IR: $\tilde{\nu}$ = 3588 m cm^{-1}, 3517 br, 3388 br, 3300 m, 3285 m, 3251 m, 3169 m, 2950 w, 2936 w, 2884 w, 2085 s, 2056 s, 1608 m, 1471 m, 1228 w, 1190 w, 1136 w, 1104 w, 1068 w, 1047 w, 1030 w, 667 br, 583 m, 462 br, 398 br.

3: Yield: 0.90 g (30%). $C_{12}H_{30}CuFeN_{10}O_4$ (497.82): calcd. C 28.95, H 6.07, Cu 12.76, Fe 11.22, N 28.14; found C 28.83, H 6.18, Cu 12.90, Fe 10.99, N 28.07. IR: $\tilde{\nu}$ = 3519 m cm^{-1}, 3384 br, 3277 s, 3235 s, 3166 m, 3014 br, 2979 m, 2888 m, 2819 m, 2705 w, 2613 w, 2526 w, 2492 w, 2095 s, 2060 s, 2032 s, 1685 w, 1660 w, 1618 w, 1604 m, 1497 m, 1477 w, 1411 w, 1335 w, 1242 w, 1214 m, 1144 w, 1102 w, 1062 w, 1038 w, 1004 w, 950 w, 754 m, 659 w, 584 m, 493 br, 419 w.

Synthesis of $[\{Cu^{II}(tn)\}_3\{Cr^{III}(CN)_6\}_2]\cdot 3H_2O$ (4): This compound was prepared as blue crystals by a procedure similar to that given below for **5**, from $(Et_4N)_3[Cr^{III}(CN)_6]$ (3.59 g, 6.0 mmol) instead of $(Et_4N)_3[Co^{III}(CN)_6]$. This procedure and analytical data have been previously communicated.[10d] Yield: 1.06 g (40%). IR: $\tilde{\nu}$ = 3627 m cm^{-1}, 3482 br, 3359 m, 3323 m, 3243 m, 3159 m, 2952 w, 2892 w, 2175 s, 2149 w, 2128 w, 1595 m, 1462 w, 1445 w, 1407 w, 1278 w, 1250 w, 1161 s, 1143 m, 1106 w, 1075 w, 1033 w, 1013 m, 914 m, 885 w, 677 w, 614 w, 493 s, 466 s, 378 m, 354 m.

Synthesis of $[\{Cu^{II}(tn)\}_3\{Co^{III}(CN)_6\}_2]\cdot 3H_2O$ (5): Under aerobic conditions, 1,3-diaminopropane (1.0 mL, 12.0 mmol) was slowly

Table 5. Crystallographic data and structural refinement parameters for compounds **1**–**5**.

	1	**2**	**3**	**4**	**5**
Empirical formula	$C_{12}H_{30}ClCu_2FeKN_{10}O_5$	$C_{12}H_{28}Cu_2FeN_{10}O_4$[a]	$C_{12}H_{30}FeCuN_{10}O_4$[a]	$C_{21}H_{36}Cr_2Cu_3N_{18}O_3$[a]	$C_{21}H_{36}Co_2Cu_3N_{18}O_3$[a]
Formula mass	651.92	559.38	497.82	883.30	897.13
Crystal system	monoclinic	monoclinic	monoclinic	orthorhombic	orthorhombic
Space group	$P2_1/c$	$P2_1/n$	$P2_1/n$	$Pbcn$	$Pbcn$
a [Å]	15.1478(3)	7.5721(11)	10.0586(4)	23.1148(4)	22.5404(3)
b [Å]	14.6941(4)	10.7215(14)	9.0189(3)	11.1692(6)	10.9865(5)
c [Å]	12.6533(4)	12.9266(18)	11.9833(6)	14.650(1)	14.2610(8)
α [°]	90	90	90	90	90
β [°]	109.95(9)	90.013(12)	104.2(1)	90	90
γ [°]	90	90	90	90	90
V [Å^3]	2647(1)	1049.4(3)	1053.8(6)	3782.2(3)	3531.6(4)
D_c [g cm^{-3}]	1.64	1.77	1.57	1.55	1.69
Z	4	2	2	4	4
μ [cm^{-1}]		27.31	17.38		27.54
Refl. measured		7909	4772		17553
Refl. unique/R_{int}		2150/0.039	2665/0.044		5888/0.063
Refl. with $I > n\sigma(I)$		1706 (n = 2)	1030 (n = 2.5)		2345 (n = 4)
Nv		147	190		218
R[b]		0.033	0.036		0.032
R_w[c]		0.060(F_o^2)	0.039(F_o)		0.038(F_o)
GooF[d]		0.915	1.024		1.122
$\Delta\rho_{max}/\Delta\rho_{min}$ [e Å^{-3}]		+0.779/–0.556	+0.311/–0.536		+0.440/–0.747

[a] The asymmetric unit contains 0.5 of the chemical formula. [b] $R = \Sigma||F_o| - |F_c||/\Sigma|F_o|$. [c] $R_w(F_o) = \{\Sigma[w(F_o - F_c)^2]/\Sigma[w(F_o)^2]\}^{1/2}$, $R_w(F_o^2) = wR_2 = \{\Sigma[w(F_o^2 - F_c^2)^2]/\Sigma[w(F_o^2)^2]\}^{1/2}$. [d] GooF = $S = \{\Sigma[w(F_o^2 - F_c^2)^2]/(N_{obsd.} - N_{var})\}^{1/2}$.

added with stirring to a concentrated aqueous solution of $CuCl_2{\cdot}2H_2O$ (2.05 g, 12.0 mmol). A concentrated aqueous solution of NaOH (0.48 g, 12.0 mmol) was then added leading to a clear solution, which was boiled for five minutes and then filtered. An aqueous solution of $(Et_4N)_3[Co^{III}(CN)_6]$ (3.63 g, 6.0 mmol) was then added to the resulting blue filtrate. Slow concentration of this solution at room temp. afforded **5** as blue crystals, which were filtered and air dried. Yield: 1.48 g (55%). $C_{21}H_{36}Co_2Cu_3N_{18}O_3$ (897.13): calcd. C 28.11, H 4.04, Co 13.14, Cu 21.25, N 28.10; found C 27.98, H 4.22, Co 12.97, Cu 21.32, N 28.01. IR: $\tilde{\nu}$ = 3618 w cm^{-1}, 3466 br, 3366 m, 3321 m, 3232 m, 3154 m, 2953 w, 2892 w, 2175 s, 2135 m, 2125 w, 1586 m, 1458 w, 1447 w, 1407 w, 1278 w, 1259 w, 1162 s, 1143 w, 1109 w, 1077 w, 1036 w, 1013 m, 913 m, 885 w, 681 w, 668 w, 493 s, 463 s, 447 m, 433 m, 418 br.

X-ray Crystallography: Data for **2** were collected on an Xcalibur 1 diffractometer (Oxford Diffraction) at 180 K whereas the data for all other compounds were collected at 288 K on an Xcalibur 2 Diffractometer (Oxford Diffraction). The structures were solved by direct methods and successive Fourier difference syntheses, and were refined on F^2 by weighted anisotropic full-matrix least-squares methods.[30] The crystal used for compound **2** presented a pseudo-merohedral twinning with a monoclinic cell having a β angle of nearly 90°, which emulates an orthorhombic cell with possible space group $Pmn2_1$. The structure was solved and refined using the $P2_1/n$ monoclinic space and the following twinning law: 1 0 0 0 –1 0 0 0 –1. The two components were in the ratio 0.53/0.46, which explains the pseudo-orthorhombic symmetry.

The hydrogen atoms of **1**, **2**, **4**, and **5** were calculated [d(C–H) = 0.95 Å], except for the hydrogen atoms of the water molecules of **1**, **4**, and **5**; the thermal parameters were taken as $U_{iso} = 1.3\,U_{equ}$(C) and therefore included as isotropic fixed contributors to F_c. For compound **3**, all hydrogen atoms were located in the difference Fourier map and were refined isotropically. Scattering factors and corrections for anomalous dispersion were taken from the International Tables for X-ray Crystallography.[31] The thermal ellipsoid drawings were made with the ORTEP program.[32] All calculations were performed on an Alphastation 255 4/233 computer. Pertinent crystallographic data and structural refinement parameters are listed in Table 5. CCDC-175834, -274145, -275481, -175842, and -275482 (for **1**–**5**, respectively) contain the supplementary crystallographic data for this paper. These data can be obtained free of charge from The Cambridge Crystallographic Data Centre via www.ccdc.cam.ac.uk/data_request/cif.

Acknowledgments

The authors gratefully acknowledge the CNRS (Centre National de la Recherche Scientifique) and the framework of a French–Spanish Integrated Action (PICASSO 2004, no. 07137XK and HF2003-258) for financial support. FT thanks the Ministère de l'Education Nationale, de la Recherche et de la Technologie for a thesis grant.

[1] a) S. M. Holmes, G. S. Girolami, *J. Am. Chem. Soc.* **1999**, *121*, 5593–5594; b) O. Hatlevik, W. E. Buschmann, J. Zhang, J. L. Manson, J. S. Miller, *Adv. Mater.* **1999**, *11*, 914–918; c) E. Dujardin, S. Ferlay, X. Phan, C. Desplanches, C. Cartier dit Moulin, P. Sainctavit, F. Baudelet, F. Dartyge, P. Veillet, M. Verdaguer, *J. Am. Chem. Soc.* **1998**, *120*, 11347–11352; d) M. Vergaguer, *Science* **1996**, *272*, 698–699; e) W. R. Entley, G. S. Girolami, *Science* **1995**, *268*, 397–400; f) S. Ferlay, T. Mallah, R. Ouahes, P. Veillet, M. Verdaguer, *Nature* **1995**, *378*, 701–703.

[2] M. Pilkington, S. Decurtins, *Comprehensive Coordination Chemistry II*, vol. 7 (Eds.: J. A. McCleverty, T. J. Meyer), Pergamon Press, Oxford, **2004**, pp. 177–229.

[3] For examples of photomagnetic materials and molecular spin devices, see: a) T. Hozumi, K. Hashimoto, S.-I. Ohkoshi, *J. Am. Chem. Soc.* **2005**, *127*, 3864–3869, and references cited therein; b) A. Dei, *Angew. Chem.* **2005**, *117*, 1184–1187; *Angew. Chem. Int. Ed.* **2005**, *44*, 1160–1163; c) V. Escax, C. Cartier dit Moulin, F. Villain, G. Champion, J.-P. Itié, P. Münsch, M. Verdaguer, A. Bleuzen, *C. R. Chim.* **2003**, *6*, 1165–1173; d) O. Sato, *Acc. Chem. Res.* **2003**, *36*, 692–700; e) Y. Arimoto, S.-I. Ohkoshi, Z. J. Zhong, H. Seino, Y. Mizobe, K. Hashimoto,

J. Am. Chem. Soc. **2003**, *125*, 9240–9241; f) S. Ohkoshi, K. Hashimoto, *J. Photochem. Photobiol., C* **2001**, *2*, 71–88; g) C. Cartier dit Moulin, F. Villain, A. Bleuzen, M.-A. Arrio, P. Sainctavit, C. Lomenech, V. Escax, F. Baudelet, E. Dartyge, J.-J. Gallet, M. Verdaguer, *J. Am. Chem. Soc.* **2000**, *122*, 6653–6658; h) O. Sato, Y. Einaga, A. Fujishima, K. Hashimoto, *Inorg. Chem.* **1999**, *38*, 4405–4412; i) Z.-Z. Gu, O. Sato, T. Iyoda, K. Hashimoto, A. Fujishima, *Chem. Mater.* **1997**, *9*, 1092–1097.

[4] O. Sato, T. Kawakami, M. Kimura, S. Hishiya, S. Kubo, Y. Einaga, *J. Am. Chem. Soc.* **2004**, *126*, 13176–13177.

[5] M. J. Scott, R. H. Holm, *J. Am. Chem. Soc.* **1994**, *116*, 11357–11367.

[6] a) S. S. Kaye, J. R. Long, *J. Am. Chem. Soc.* **2005**, *127*, 6506–6507; b) L. G. Beauvais, J. R. Long, *J. Am. Chem. Soc.* **2002**, *124*, 12096–12097.

[7] W. Dong, L.-N. Zhu, H.-B. Song, D.-Z. Liao, Z.-H. Jiang, S.-P. Yan, P. Cheng, S. Gao, *Inorg. Chem.* **2004**, *43*, 2465–2467.

[8] a) M. Ohba, H. Okawa, *Coord. Chem. Rev.* **2000**, *198*, 313–328, and references cited therein; b) M. K. Saha, M. C. Morón, F. Palacio, I. Bernal, *Inorg. Chem.* **2005**, *44*, 1354–1361; c) H.-Z. Kou, B. C. Zhou, S. Gao, D.-Z. Liao, R.-J. Wang, *Inorg. Chem.* **2003**, *42*, 5604–5611; d) E. Colacio, J. M. Domínguez-Vera, F. Lloret, A. Rodríguez, H. Stoeckli-Evans, *Inorg. Chem.* **2003**, *42*, 6962–6964; e) H.-Z. Kou, B. C. Zhou, D.-Z. Liao, R.-J. Wang, Y. Li, *Inorg. Chem.* **2002**, *41*, 6887–6891; f) F. Bellouard, M. Clemente-León, E. Coronado, J. R. Galán-Mascarós, C. J. Gómez-García, F. M. Romero, K. R. Dunbar, *Eur. J. Inorg. Chem.* **2002**, 1603–1606; g) E. Coronado, C. J. Gómez-García, A. Nuez, F. M. Romero, E. Rusanov, H. Stoeckli-Evans, *Inorg. Chem.* **2002**, *41*, 4615–4617; h) K. Inoue, H. Imai, P. S. Ghalsasi, K. Kikuchi, M. Ohba, H. Okawa, J. V. Yakhmi, *Angew. Chem.* **2001**, *113*, 4372–4375; *Angew. Chem. Int. Ed.* **2001**, *40*, 4242–4245; i) J. A. Smith, J.-R. Galán-Mascarós, R. Clérac, K. R. Dunbar, *Chem. Commun.* **2000**, 1077–1078.

[9] a) E. Coronado, C. Gimenez-Saiz, A. Nuez, V. Sánchez, F. M. Romero, *Eur. J. Inorg. Chem.* **2003**, 4289–4293; b) E. Coronado, C. Giménez-Saiz, J. M. Martinez-Agudo, A. Nuez, F. M. Romero, H. Stoeckli-Evans, *Polyhedron* **2003**, *22*, 2435–2440; c) F. Thétiot, S. Triki, J. Sala-Pala, *New J. Chem.* **2002**, *26*, 196–198; d) T. Lu, H. Xiang, S. Chen, C. Su, K. Yu, Z. Mao, P. Cheng, L. Ji, *J. Inorg. Organomet. Polym.* **1999**, *9*, 165–178; e) H.-Z. Kou, D.-Z. Liao, P. Cheng, Z.-H. Jiang, S.-P. Yan, G.-L. Wang, X.-K. Yao, H.-G. Wang, *J. Chem. Soc., Dalton Trans.* **1997**, 1503–1506.

[10] a) X.-P. Shen, S. Gao, G. Yin, K.-B. Yu, Z. Xu, *New J. Chem.* **2004**, *28*, 996–999; b) H.-Z. Kou, Y.-B. Jiang, B. C. Zhou, R.-J. Wang, *Inorg. Chem.* **2004**, *43*, 3271–3276; c) M. S. El Fallah, J. Ribas, X. Solans, M. Font-Bardia, *New J. Chem.* **2003**, *27*, 895–898; d) F. Thétiot, S. Triki, J. Sala-Pala, C. J. Gómez-García, S. Golhen, *Chem. Commun.* **2002**, 1078–1079; e) H.-Z. Kou, S. Gao, J. Zhang, G.-H. Wen, G. Su, R. K. Zheng, X. X. Zhang, *J. Am. Chem. Soc.* **2001**, *123*, 11809–11810.

[11] a) C. P. Berlinguette, A. Draguescu-Andrasi, A. Sieber, H.-U. Güdel, C. Achim, K. R. Dunbar, *J. Am. Chem. Soc.* **2005**, *127*, 6766–6779; b) C. P. Berlinguette, A. Draguescu-Andrasi, A. Sieber, J. R. Galán-Mascarós, H.-U. Güdel, C. Achim, K. R. Dunbar, *J. Am. Chem. Soc.* **2004**, *126*, 6222–6223; c) H.-Z. Kou, B. C. Zhou, S.-F. Si, R.-J. Wang, *Eur. J. Inorg. Chem.* **2004**, 401–408; d) H. J. Choi, J. J. Sokol, J. R. Long, *Inorg. Chem.* **2004**, *43*, 1606–1608; e) R. Tiron, W. Wernsdorfer, F. Tuyeras, A. Scuiller, V. Marvaud, M. Verdaguer, *Polyhedron* **2003**, *22*, 2427–2433; f) V. Marvaud, C. Decroix, A. Scuiller, F. Tuyèras, C. Guyard-Duhayon, J. Vaissermann, J. Marrot, F. Gonnet, M. Verdaguer, *Chem. Eur. J.* **2003**, *9*, 1692–1705; g) R. J. Parker, K. D. Lu, S. R. Batten, B. Moubaraki, K. S. Murray, L. Spiccia, J. D. Cashion, A. D. Rae, A. C. Willis, *J. Chem. Soc., Dalton Trans.* **2002**, 3723–3730; h) K. E. Vostrikova, D. Luneau, W. Wernsdorfer, P. Ray, M. Verdaguer, *J. Am. Chem. Soc.* **2000**, *122*, 718–719; i) D. G. Fu, J. Chen, X. S. Tan, L. J. Jiang, S. W. Zhang, P. J. Zheng, W. X. Tang, *Inorg. Chem.* **1997**, *36*, 220–225.

[12] a) R. Lescouëzec, J. Vaissermann, L. M. Toma, R. Carrasco, F. Lloret, M. Julve, *Inorg. Chem.* **2004**, *43*, 2234–2236; b) L. M. Toma, F. S. Delgado, C. Ruiz-Pérez, R. Carrasco, J. Cano, F. Lloret, M. Julve, *Dalton Trans.* **2004**, *18*, 2836–2846; c) Y.-Z. Zhang, S. Gao, H.-L. Sun, G. Su, Z.-M. Wang, S. W. Zhang, *Chem. Commun.* **2004**, 1906–1907; d) R. Lescouëzec, J. Vaissermann, C. Ruiz-Pérez, F. Lloret, R. Carrasco, M. Julve, M. Verdaguer, Y. Dromzee, D. Gatteschi, W. Wernsdorfer, *Angew. Chem.* **2003**, *115*, 1521–1524; *Angew. Chem. Int. Ed.* **2003**, *42*, 1483–1486; e) L. M. Toma, R. Lescouëzec, F. Lloret, M. Julve, J. Vaissermann, M. Verdaguer, *Chem. Commun.* **2003**, 1850–1851; f) R. Lescouëzec, F. Lloret, M. Julve, J. Vaissermann, M. Verdaguer, R. Llusar, S. Uriel, *Inorg. Chem.* **2001**, *40*, 2065–2072; g) W.-F. Yeung, W.-L. Man, W.-T. Wong, T.-C. Lau, S. Gao, *Angew. Chem.* **2001**, *113*, 3121–3123; *Angew. Chem. Int. Ed.* **2001**, *40*, 3031–3033; h) N. Matsumoto, Y. Sunatsuki, H. Miyasaka, Y. Hashimoto, D. Luneau, J.-P. Tuchagues, *Angew. Chem.* **1999**, *111*, 137–139; *Angew. Chem. Int. Ed.* **1999**, *38*, 171–173.

[13] a) Z.-H. Ni, H.-Z. Kou, Y.-H. Zhao, L. Zheng, R.-J. Wang, A.-L. Cui, O. Sato, *Inorg. Chem.* **2005**, *44*, 2050–2059; b) S. Wang, J.-L. Zuo, H.-C. Zhou, Y. Song, S. Gao, X.-Z. You, *Eur. J. Inorg. Chem.* **2004**, 3681–3687; c) S. Wang, J.-L. Zuo, S. Gao, Y. Song, H.-C. Zhou, Y.-Z. Zhang, X.-Z. You, *J. Am. Chem. Soc.* **2004**, *126*, 8900–8901; d) H. Oshio, H. Onodera, T. Ito, *Chem. Eur. J.* **2003**, *9*, 3946–3950; e) J. Y. Yang, M. P. Shores, J. J. Sokol, J. R. Long, *Inorg. Chem.* **2003**, *42*, 1403–1419; f) M. P. Shores, J. J. Sokol, J. R. Long, *J. Am. Chem. Soc.* **2002**, *124*, 2279–2292; g) R. Lescouëzec, F. Lloret, M. Julve, J. Vaissermann, M. Verdaguer, *Inorg. Chem.* **2002**, *41*, 818–826; h) H. Oshio, M. Yamamoto, T. Ito, *Inorg. Chem.* **2002**, *41*, 5817–5820; i) J. J. Sokol, M. P. Shores, J. R. Long, *Angew. Chem.* **2001**, *113*, 242–245; *Angew. Chem. Int. Ed.* **2001**, *40*, 236–239.

[14] a) J.-E. Koo, D.-H. Kim, Y.-S. Kim, Y. Do, *Inorg. Chem.* **2003**, *42*, 2983–2987; b) R. J. Parker, L. Spiccia, B. Moubaraki, K. S. Murray, D. C. R. Hockless, A. D. Rae, A. C. Willis, *Inorg. Chem.* **2002**, *41*, 2489–2495; c) J. A. Smith, J. R. Galán-Mascarós, R. Clérac, J.-S. Sun, X. Ouyang, K. R. Dunbar, *Polyhedron* **2001**, *20*, 1727–1734; d) X. Sun, Z. Wang, Z. Chen, J. Bian, C. Yan, G. Xu, *Prog. Nat. Sc.* **1999**, *9*, 425–431; e) J. Zou, X. Hu, C. Duan, Z. Xu, X. You, *Transition Met. Chem. (Dordrecht, Neth.)* **1998**, *23*, 477–480; f) R. J. Parker, D. C. R. Hockless, B. Moubaraki, K. S. Murray, L. Spiccia, *Chem. Commun.* **1996**, 2789–2790.

[15] *Stability Constants of Metal-Ion Complexes. Part B: Organic ligands*, IUPAC Chemical Data Series, no. 22, Pergamon Press, Oxford, **1979**, p. 122.

[16] S. M. Nelson, *Comprehensive Coordination Chemistry*, vol. 4 (Eds.: G. Wilkinson, R. D. Gillard, J. A. McCleverty), Pergamon Press, Oxford, **1987**, pp. 217–267.

[17] A. G. Sharpe, *Comprehensive Coordination Chemistry*, vol. 2 (Eds.: G. Wilkinson, R. D. Gillard, J. A. McCleverty), Pergamon Press, Oxford, **1987**, pp. 7–14.

[18] a) I. Bertini, C. Luchinat, F. Mani, A. Scozzafava, *Inorg. Chem.* **1980**, *19*, 1333–1336; b) J. A. Fee, *Struct. Bonding (Berlin)* **1975**, *23*, 1–60; c) W. U. Malik, S. I. Ali, *Bull. Chem. Soc. Jpn.* **1961**, *34*, 1310–1313.

[19] K. Nakamoto, *Infrared and Raman Spectra of Inorganic and Coordination Compounds*, 4th ed., Wiley-Interscience, New York, **1978**.

[20] R. J. Parker, L. Spiccia, S. R. Batten, J. D. Cashion, G. D. Fallon, *Inorg. Chem.* **2001**, *40*, 4696–4704.

[21] a) M. J. Scott, S. C. Lee, R. H. Holm, *Inorg. Chem.* **1994**, *33*, 4651–4662; b) G. O. Morpurgo, V. Mosini, P. Porta, G. Dessy, V. Fares, *J. Chem. Soc., Dalton Trans.* **1981**, 111–117.

[22] P. V. Bernhardt, B. D. Macpherson, M. Martinez, *Inorg. Chem.* **2000**, *39*, 5203–5208.

[23] a) N. Mondal, M. K. Saha, B. Bag, S. Mitra, V. Gramlich, J. Ribas, M. S. El Fallah, *J. Chem. Soc., Dalton Trans.* **2000**, 1601–1604; b) J. Luo, M. Hong, C. Chen, M. Wu, D. Gao, *Inorg. Chim. Acta* **2002**, *328*, 185–190.
[24] a) W. Addison, T. N. Rao, J. Reedijk, J. van Rijn, G. C. Verschoor, *J. Chem. Soc., Dalton Trans.* **1984**, 1349–1356; b) M. Vaidyanathan, R. Balamurugan, U. Sivagnanam, M. Palaniandavar, *J. Chem. Soc., Dalton Trans.* **2001**, 3498–3506.
[25] M. Ohba, N. Usuki, N. Fukita, H. Okawa, *Angew. Chem.* **1999**, *111*, 1911–1914; *Angew. Chem. Int. Ed.* **1999**, *38*, 1795–1798.
[26] a) C. S. Hong, Y. S. You, *Inorg. Chim. Acta* **2004**, *357*, 3271–3278; b) N. Mondal, M. K. Saha, B. Bag, S. Mitra, G. Rosair, M. S. El Fallah, *Polyhedron* **2001**, *20*, 579–584; c) Z. Travnicek, Z. Smékal, A. Escuer, J. Marek, *New J. Chem.* **2001**, *25*, 655–658; d) F. Bellouard, M. Clemente-León, E. Coronado, J. R. Galán-Mascarós, C. Giménez-Saiz, C. J. Gómez-García, T. Woike, *Polyhedron* **2001**, *20*, 1615–1619; e) E. Colacio, J. M. Domínguez-Vera, M. Ghazi, R. Kivekäs, J. M. Moreno, A. Pajunen, *J. Chem. Soc., Dalton Trans.* **2000**, 505–509; f) H. Oshio, O. Tamada, H. Onodera, T. Ito, T. Ikoma, S. Tero-Kubota, *Inorg. Chem.* **1999**, *38*, 5686–5689; g) H.-Z. Kou, H.-M. Wang, D.-Z. Liao, P. Cheng, Z.-H. Jiang, S.-P. Yan, X.-Y. Huang, G.-L. Wang, *Aust. J. Chem.* **1998**, *51*, 661–665; h) C. Q. Liu, J. M. Shi, W. Xu, W. Xu, Y. Q. Chen, *Pol. J. Chem.* **2003**, *77*, 929–933; i) H. L. Shyu, H.-H. Wei, *J. Coord. Chem.* **1999**, *47*, 319–330; j) J. Zou, Z. Xu, X. Huang, W.-L. Zhang, X.-P. Shen, Y.-P. Yu, *J. Coord. Chem.* **1997**, *42*, 55–61.
[27] a) M. K. Saha, F. Lloret, I. Bernal, *Inorg. Chem.* **2004**, *43*, 1969–1975; b) C. R. Choudhury, S. K. Dey, S. Mitra, N. Mondal, J. Ribas, K. M. Malik, *Bull. Chem. Soc. Jpn.* **2004**, *77*, 959–964; c) V. Marvaud, C. Decroix, A. Scuiller, C. Guyard-Duhayon, J. Vaissermann, F. Gonnet, M. Verdaguer, *Chem. Eur. J.* **2003**, *9*, 1678–1691; d) B. Li, X. Shen, K. Yu, Z. Xu, *J. Coord. Chem.* **2002**, *55*, 1191–1198; e) N. Mondal, D. K. Dey, S. Mitra, V. Gramlich, *Polyhedron* **2001**, *20*, 607–613; f) M. Ferbinteanu, S. Tanase, M. Andruh, Y. Journaux, F. Cimpoesu, I. Strenger, E. Rivière, *Polyhedron* **1999**, *18*, 3019–3025.
[28] N. Fukita, M. Ohba, H. Okawa, K. Matsuda, H. Iwamura, *Inorg. Chem.* **1998**, *37*, 842–848.
[29] P. Le Magueres, PhD Thesis, **1995**, University of Rennes 1, France.
[30] a) C. K. Fair, *MolEN, An Interactive Intelligent System for Crystal Structure Analysis*, User Manual, **1985**, Enraf-Nonius, Delft, The Netherlands; b) G. M. Sheldrick, SHELX97. Programs for Crystal Structure Analysis, **1997**, University of Göttingen, Germany.
[31] *International Tables for X-ray Crystallography*, vol. 4, Kynoch Press, Birmingham, **1975**.
[32] C. K. Johnson, *ORTEP*, Rep. ONL-3794, Delft, The Netherlands, **1985**.

Received: June 24, 2005
Published Online: November 21, 2005

